International Journal of Mass Spectrometry 277 (2008) 279–283

Contents lists available at ScienceDirect

International Journal of Mass Spectrometry

journal homepage: www.elsevier.com/locate/ijms

Interaction of slow electrons with methyl phosphate esters

Carl Winstead*, Vincent McKoy

A.A. Noyes Laboratory of Chemical Physics, California Institute of Technology, Pasadena, CA 91125, USA

ARTICLE INFO

Article history:
Received 13 March 2008
Received in revised form 16 April 2008
Accepted 21 April 2008
Available online 1 May 2008

PACS:
34.80.Bm
34.80.Ht

Keywords:
Phosphoric acid
Methyl phosphate
Electron scattering
Shape resonance
Dissociative attachment

ABSTRACT

We report computed cross sections for low-energy elastic collisions of electrons with the methyl esters of phosphoric acid, monomethyl, dimethyl, and trimethyl phosphate, and with phosphoric acid itself. For phosporic acid and monomethyl phosphate, polarization effects are included in the calculation, while the two larger molecules are treated in the static-exchange approximation, that is, with polarization neglected. The integral elastic cross sections exhibit broad shape resonances above 5 eV that give rise to strong variations in the differential cross section with energy. However, no shape resonances are evident below 5 eV. We compare our results to previous calculations and measurements and discuss their relevance to electron-induced damage to the DNA backbone.

1. Introduction

Much attention has been devoted to investigating the mechanisms by which slow electrons break DNA strands (for a recent review, see [1]). Though the site of breakage appears to be quite specific, namely the phosphoesteric bonds connecting C 3′ or C 5′ of deoxyribose to the phosphate group [2], the initial site of electron capture may nonetheless be elsewhere. In the model advanced by Simons and co-workers [3–6], electrons are initially trapped in empty π^* orbitals of the nucleobases to form metastable anions (elastic shape resonances, in scattering terminology) and then undergo intramolecular transfer to the backbone, where they localize in a C 5′–O σ^* orbital and thus lead to bond breaking at that site. This model has received implicit support from work that shows a correlation between nucleobase shape-resonance energies and the observed pattern of single-strand breaks in thin-film DNA [9]. However, in light of the limited information so far available, direct attachment of electrons to the DNA backbone has also been suggested [7,8] and is by no means ruled out as a competing, if not the primary, mechanism of strand breaking. Several recent studies have, therefore, addressed the possibility of direct electron attachment to the DNA backbone. Among these, we mention in particular the experiments of Illenberger and coworkers, who have studied gas-phase dissociative attachment (DA) to deoxyribose analogues [10–12] and to the phosphoric acid esters dibutyl phosphate and triethyl phosphate [13]. In the latter study, DA to dibutyl phosphate was observed to produce a number of phosphorous-containing anionic fragments, as well as one in which an entire neutral butyl group had been removed. Such processes, if operable in DNA itself, would lead to strand breaks.

In the present work, we use first-principles computational methods to study the interaction of slow electrons with three simple model compounds containing phosphoesteric bonds, (mono)methyl phosphate (hereafter MMP), dimethyl phosphate (DMP), and trimethyl phosphate (TMP), as well as with their parent compound, phosphoric acid, H_3PO_4. We are particularly interested in identifying any shape resonances that may be present in the elastic electron-scattering cross sections, because temporary trapping in such resonances may promote DA and other energy-deposition processes. Although no electron-collision data for MMP or DMP are, to our knowledge, available, recently Aflatooni et al. [14] have reported DA measurements for TMP, while Burrow et al. [15] have reported electron transmission measurements for TMP. Our results may also be compared to the DA measurements on dibutyl and triethyl phosphate mentioned above [13], as well as to elastic cross section calculations on H_3PO_4 [16] and DA measurements on thin films of the salt NaH_2PO_4 [17].

* Corresponding author.
E-mail address: carl@schwinger.caltech.edu (C. Winstead).

1387-3806/$ – see front matter © 2008 Elsevier B.V. All rights reserved.
doi:10.1016/j.ijms.2008.04.015

2. Computational details

We optimized the geometries of H_3PO_4, MMP, DMP, and TMP at the level of second-order Möller-Plesset perturbation theory in the 6-31 G(d) basis set using GAMESS [18]. Because various conformers appear plausible, we tested several different starting geometries for H_3PO_4 and MMP in an effort to locate the respective global minima. Our lowest energy results were geometries in which the hydroxy and methoxy groups are all *gauche* to the phosphoryl bond, and these structures were used in the electron-scattering calculations. We likewise used all-*gauche* geometries for DMP and TMP. The conformers adopted for H_3PO_4 and TMP have C_3 point-group symmetry, while those used for MMP and DMP have C_1 (i.e., no) symmetry. Other conformers of H_3PO_4 and MMP were nearly as low in energy as the all-*gauche* forms (within $\approx$ 2 millihartree), and it is likely all four molecules exist in the gas phase as mixtures of conformers. Although the forward scattering may be significantly affected by the molecular conformation, inasmuch as the net static electric dipole moment is quite sensitive to the orientation of the hydroxyl and esteric bonds, we do not expect the precise molecular conformation to strongly affect the resonance structure of the cross sections that is our main interest.

Scattering calculations were carried out using the Schwinger multichannel (SMC) method [19,20] as implemented for parallel computers [21]. A description of the SMC method may be found in the indicated references; here we give only details specific to the present calculations. For all four molecules, we carried out static-exchange (SE) calculations, that is, calculations in which we neglected the response of the molecular charge density to the presence of the projectile electron ("polarization"). These SE calculations used the TZV (triple-zeta valence) basis set contained in GAMESS together with a (1s1p3d,1s2p) supplement. The $(x^2 + y^2 + z^2)$ linear combination of Gaussian d orbitals was excluded, and GAMESS default values were used for all exponents and splitting factors. The target molecule was described at the Hartree–Fock level, and all virtual orbitals were antisymmetrized with the N-electron target wavefunction to form an $(N + 1)$-electron doublet variational space for the scattering calculation.

For the smaller molecules, H_3PO_4 and MMP, we also carried out static-exchange plus polarization (SEP) calculations. The SEP calculation on H_3PO_4 employed the aug-cc-pVDZ basis set as contained in GAMESS, while the MMP SEP calculation employed the the DZV (double-zeta valence) basis set contained in GAMESS with a 1s1p2d supplement of diffuse and polarization functions on the heavy atoms and a 1s1p supplement on the hydrogens, again using default exponents and splitting factors; in both cases the "3s" combinations of d Gaussians were excluded. To represent polarization effects, the $(N + 1)$-electron variational space was expanded to include doublet configurations built on singlet-coupled single excitations from valence orbitals to low-lying modified virtual orbitals (MVOs) [22] that were formed using a +6 cationic core. Because such MVOs are compact and valence-like, their use as particle orbitals accelerates the convergence of the configuration expansion. For H_3PO_4 we included singlet excitations from the 6 outermost occupied orbitals into the 15 lowest MVOs, each antisymmetrized with one of the 100 lowest energy MVOs to form a doublet configuration state function (CSF), as well as singlet excitations from the next 6 more tightly bound occupied orbitals into the 10 lowest MVOs, antisymmetrized with the 50 lowest MVOs to form doublet CSFs. This resulted in a variational space of dimension 11,226 for the SEP calculation. For MMP, we included singlet excitations from the 15 outermost occupied orbitals into the 12 lowest MVOs, antisymmetrized with the 80 lowest energy MVOs. The resulting variational space was of dimension 13,558. As a diagnostic, we extracted SE cross sections from the SEP calculations by solving the sub-problems in which all target-excited configurations were discarded and verified that they agreed well with the TZV-basis SE results.

All of the molecules studied here are polar, and their electron scattering cross sections will consequently be affected, especially at near-forward angles, by long-range interactions of the projectile electron with the field of the permanent electric dipole. We applied a Born completion procedure described elsewhere [23] to the SEP

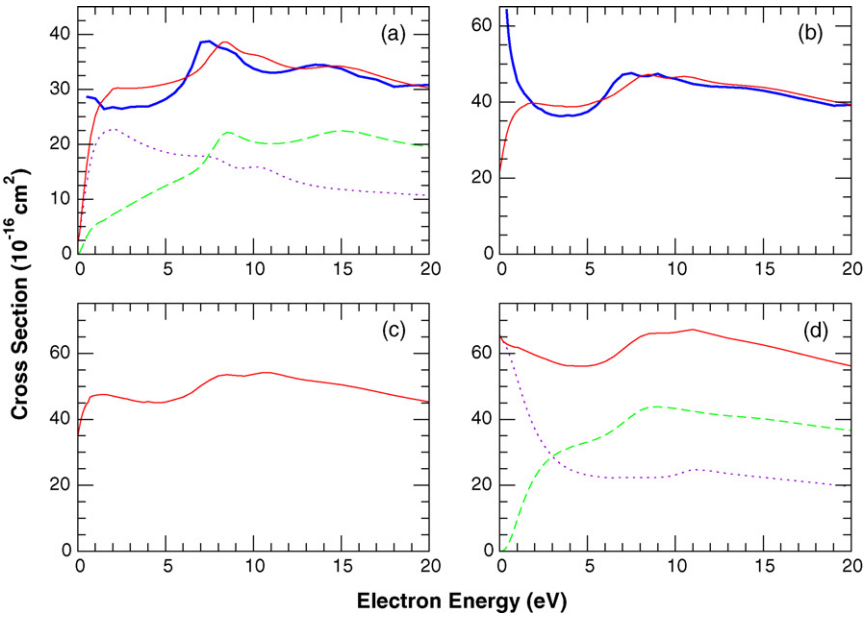

Fig. 1. Integral elastic cross sections for electron collisions with (a) H_3PO_4, (b) monomethyl phosphate, (c) dimethyl phosphate, and (d) trimethylphosphate. The heavy solid blue lines in panels (a) and (b) are computed in the SEP approximation and include the Born-dipole correction. The solid red lines are computed in the static-exchange approximation. For the molecules possessing C_3 symmetry, the static-exchange cross section is decomposed into contributions from ^{2}A (dotted violet lines) and ^{2}E (dashed green lines).

results for H_3PO_4 and MMP, using the respective Hartree–Fock dipole moments, 0.5291 and 0.9615 Debye. For both molecules, the partial-wave cutoff ℓ_{max} at which the SMC results were matched to the Born results was increased from 2 to 7 between 0.4 and 5 eV and kept at 7 above 5 eV. Integral and momentum-transfer cross sections were extracted from the corrected differential cross sections (DCS) by integration with an extended Simpson's rule, implicitly ignoring the divergence of the DCS at 0° by starting the integration at 0.1°. We did not apply a dipole-Born correction to the lower level results for DMP and TMP because the correction is most significant at the lowest energies, where the SE approximation itself becomes unreliable.

3. Results and discussion

Our calculated integral cross sections (ICS) for elastic electron scattering by H_3PO_4, MMP, DMP, and TMP are shown in Fig. 1. For DMP and TMP, only SE results are available, while for H_3PO_4 and MMP, both SE and SEP results are shown. The ICS for each molecule displays three broad maxima between about 5 and 15 eV, which we attribute to shape resonances: in the SE approximation, the first occurs at about 8.5 eV, the second at 10–11 eV, and the third and broadest at about 15 eV. As expected, the inclusion of the attractive polarization interaction shifts these peaks to lower energy; as seen in the upper two panels of Fig. 1, the shift is about 1.5 eV for all three peaks in both H_3PO_4 and MMP, and we would therefore predict comparable shifts in DMP and TMP. SEP differential cross sections for H_3PO_4 and MMP are shown at selected energies in Fig. 2, where strong variations in the angular pattern of scattering as the collision energy traverses the resonant region are evident.

The smallest and largest molecules, H_3PO_4 and TMP, possess C_3 point-group symmetry, and we were able to decompose their SE ICS into ^{2}A and ^{2}E contributions. These symmetry contributions are shown in panels (a) and (d) of Fig. 1 and give further insight into the resonance structure. In particular, we see that the lowest energy maximum in the H_3PO_4 ICS arises from overlapping peaks in ^{2}A and ^{2}E, the second maximum from ^{2}A only, and the broad peak near 15 eV from ^{2}E only. The situation in TMP is similar, except that the ^{2}A contribution to the lowest energy peak is very small or absent. The resonances in the H_3PO_4 ICS correlate fairly well with the minimal-basis-set virtual orbital energies (computed using GAMESS [18] and the "MINI" basis) shown in Table 1. In particular, the energy order of the orbitals matches that of the resonance peaks in the symmetry components of the SE ICS, and for the first three orbitals, there is also fairly close agreement with the resonance energies. TMP has many more minimal-basis virtual orbitals, but the lowest three agree closely in character and energy (within a few tenths of an eV) with those of H_3PO_4, while the fourth is an e orbital of C — O σ^* character at 14.4 eV, and thus analogous to but somewhat lower in energy than the LUMO + 3 of H_3PO_4. On the whole, then, the symmetry decomposition and comparison with minimal-basis virtual valence orbitals accounts well for the observed resonances, and the strong resemblance among the cross sections of the four molecules may be understood from the fact that the low-energy resonances involve the core phosphate group that is common to all four.

Table 1
Minimal-basis-set virtual orbital energies for H_3PO_4

Orbital	Symmetry	Character	Energy (eV)
LUMO	*a*	P —O/P=0 σ^*	8.8
LUMO + 1	*e*	P — O σ^*/P=O π^*	9.6
LUMO + 2	*a*	P=O σ^*/O — H σ^*	13.2
LUMO + 3	*e*	O — H σ^*	16.5
LUMO + 4	*a*	O — H σ^*	18.2

In Fig. 3 we compare our SEP ICS for H_3PO_4 with the result obtained by Tonzani and Greene [16]. The main qualitative difference between the two results is that the ICS of Tonzani and Greene exhibits a much larger dipole-scattering background. There is moderate agreement on the shape resonances, however: in the energy range where we see three maxima that are associated, through the symmetry decomposition discussed above, with four resonances, Tonzani and Greene see four maxima, although at somewhat different energies. On the other hand, their time-delay analysis identified only two resonances, at 7.7 and 12.5 eV, rather than four.

Limited experimental information about the resonances in the molecules studied here is available from dissociative-attachment

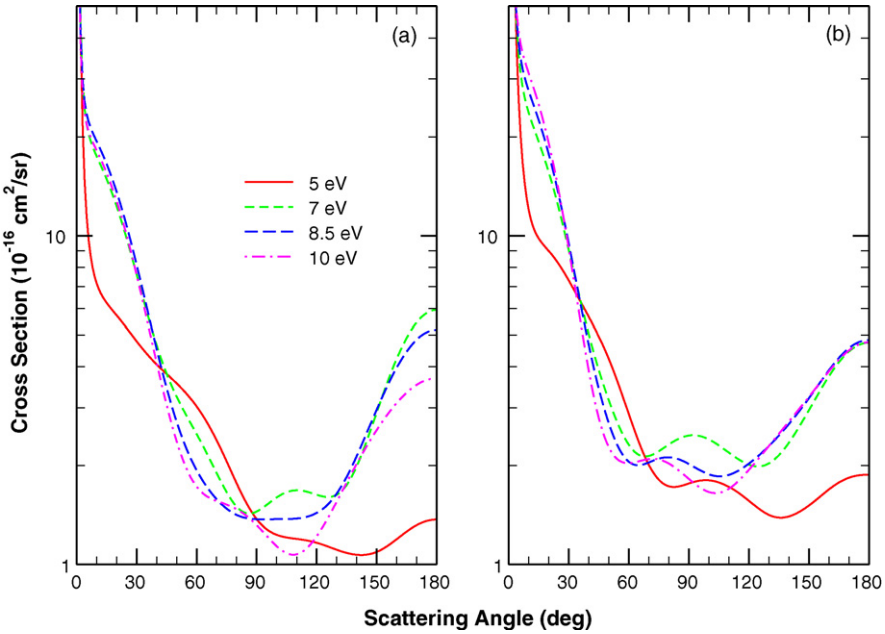

Fig. 2. Differential elastic cross sections for electron collisions with (a) H_3PO_4 and (b) monomethyl phosphate computed in the static-exchange plus polarization approximation, at selected energies as indicated in the legend.

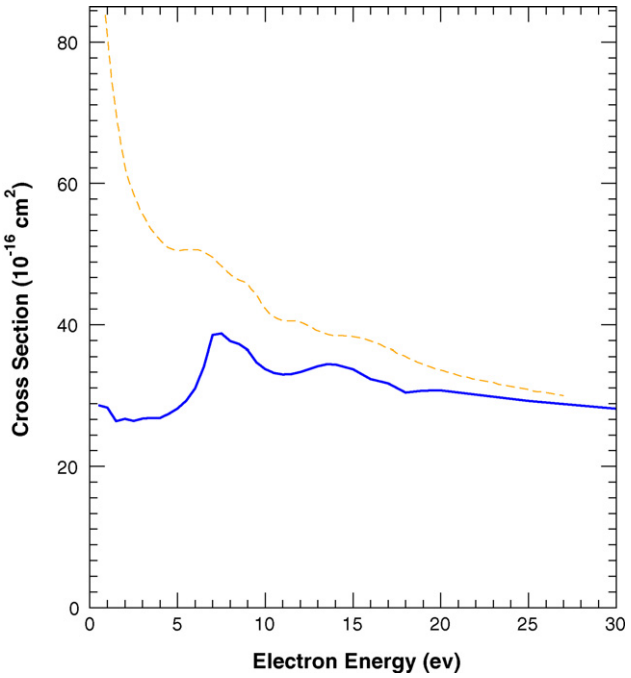

Fig. 3. Comparison of calculated elastic integral cross sections for electron scattering by H_3PO_4: present result, solid blue line; result of Ref. [16], dashed orange line.

and electron-transmission measurements. In their DA study of TMP, Aflatooni et al. [14] observed a peak at 7.4 eV which they assigned, based on its energy, to a core-excited resonance. Our elastic-scattering results, on the other hand, suggest possible assignment to a shape resonance or resonances associated with the LUMO and/or LUMO + 1. The P — O σ^* character of those orbitals would make DA to methanolate ion, CH_3O^-, appear a likely process; however, Aflatooni et al. collected the total ion current without mass resolution, so it is not possible to test this prediction. At higher energies the anion signal is overwhelmed by cations arising from electron-impact ionization, so it is not possible to compare our higher lying resonances against the DA measurements. At lower energies, the DA measurements of Aflatooni et al. [14] agree with our elastic ICS insofar as neither indicates the presence of shape resonances there. However, recent electron-transmission measurements by the same group indicate resonances at 2.1 and 4.6 eV in the TMP total scattering cross section, which they assign as shape resonances associated with low-lying valence orbitals [15]. In our view the required shifts from the static-exchange resonance positions are implausibly large, especially considering that our SEP calculations for H_3PO_4 and MMP indicate much smaller polarization shifts. Thus, although we are unable to account for the observed low-energy resonances, we do not believe them to be valence shape resonances, the lowest of which we expect to occur near 7 eV.

König et al. [13] measured DA spectra for the dibutyl and triethyl phosphate esters, observing a variety of anionic fragments. One of the principal dissociation pathways observed in dibutyl phosphate was loss of a butyl (C_4H_9) radical to form an anion of mass 153 amu, with peaks in the anion yield at 2.8 and 8 eV, while a major process in triethyl phosphate was loss of an ethoxy (C_2H_5O) radical to form a $(C_2H_5O)_2PO^-$ anion, with yield peaking near 8 eV. However, the largest yields in dibutyl phosphate were of the singly deprotonated radical anion and of OH^-, with yield curves peaking at 1.0 and 0.2 eV, respectively. König et al. assign the peaks near 8 eV to core-excited resonances involving the hydrocarbon groups and the lower energy peaks to shape resonances involving trapping in a phosphoryl π^* orbital. As discussed above, our scattering calculations on the methyl esters suggest that the lowest shape resonances lie at about 7 eV or above; because these resonances are associated with the phosphate group, it appears unlikely that they would be much affected by substituting heavier alkyl side groups for the methyls. Thus we tentatively suggest that the fragments observed near 8 eV may arise, at least in part, from valence shape resonances (or possibly from mixed resonances with partial shape-resonant character), while the origin of the DA peaks at lower energy remains unclear. However, we note that our calculations by no means rule out other mechanisms, such as electronic Feshbach resonances, that could also account for the higher energy DA features.

Pan and Sanche [17] measured DA to the monosodium salt of phosphoric acid, NaH_2PO_4, in the condensed phase, observing a single broad peak whose maximum fell at 8.8, 8.0, or 7.3 eV depending on whether the anion detected was H^-, O^-, or OH^-. The observation of an OH^- peak at 7.3 eV fits well with our prediction of a and e P — O σ^* valence shape resonances in this energy range in the H_3PO_4 elastic cross section. Likewise, the second ^2A shape resonance, which has O — H σ^* character, may account for the H^- peak at 8.8 eV. Pan and Sanche assign this feature to a core-excited rather than shape resonance. While our results provide a possible alternative, they by no means rule that assignment out; moreover, at these energies, resonances of mixed shape and core-excited character are also possible. It is less clear how to account for the production of O^-, which Pan and Sanche attribute to breaking of the phosphoryl bond due to trapping in a P=O π^* orbital. Although Table 1 indicates some π^* character for the LUMO + 1 e orbital because of the presence of a nodal plane between P and O, there is in fact little density on the phosphoryl oxygen, as seen in Fig. 4. The question of phosphoryl π^* orbitals is discussed further immediately below.

Various investigators have postulated that low-energy electrons incident on DNA or on model compounds such as the phosphoesters may be trapped in a phosphoryl π^* orbital [2,8,13,17], thereby promoting dissociation. As recently discussed in detail by Burrow et al. [15], whether there is in fact a phosphoryl π bonding orbital, and thus whether there is a conjugate π^* orbital, is problematic. Although the bond is conventionally drawn as a double bond and is

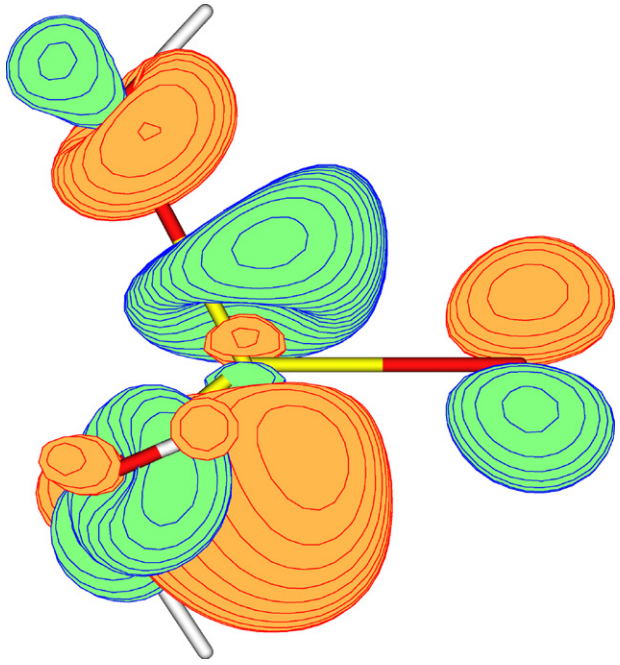

Fig. 4. Second-lowest minimal-basis Hartree–Fock virtual orbital (LUMO + 1) of H_3PO_4.

somewhat shorter than the other phosphate P — O bonds, a strong case can be made that it is better described as a coordinate covalent or dative single bond in which P shares its two lone-pair electrons with O. Indeed, none of the occupied orbitals of H_3PO_4 particularly resembles a P — O π bonding orbital, while the highest occupied orbital (HOMO) is a doubly degenerate e orbital comprising both of the O $2p_{x,y}$ lone-pair orbitals, one of which ought to form part of any such P — O π bond. Burrow et al. [15] conclude that none of the virtual orbitals in TMP or various related compounds fits the description of a phosphoryl π^* orbital, while we showed above that the LUMO + 1 of H_3PO_4, Fig. 4, has only slight phosphoryl π^* character and is better described as a P — O σ^* orbital involving the remaining oxygens.

More to the point, regardless of how one characterizes the virtual valence orbitals, we find that the resonances associated with them lie at energies typically associated with σ^* orbitals, i.e., about 7 eV or higher, and not at typical π^* resonance energies (well below 5 eV). Because the virtual orbitals associated with them are localized on the phosphate, the lowest energy resonances were seen to be insensitive to the number of methyl groups appended, and we also expect them to be insensitive to the size of the appended groups; thus we would predict similar results for the lowest energy resonances in phosphoesters formed from larger alkyls. Our conclusion here differs from that of Burrow et al. [15], who interpret the features they see at 2.1 and 4.6 eV in the TMP electron transmission spectrum as valence shape resonances; moreover, it leaves unexplained low-energy DA resonances seen in NaH_2PO_4 [17] and dibutyl phosphate [13]. The nature of those low-energy features poses an intriguing problem for future study.

Acknowledgments

This paper is respectfully dedicated to Prof. Dr. Eugen Illenberger on the occasion of his 65th birthday. We thank Prof. Paul Burrow for communicating results in advance of publication. The work reported here was supported by the Chemical Sciences, Geosciences and Biosciences Division, Office of Basic Energy Sciences, Office of Science, US Department of Energy. Use of the Jet Propulsion Laboratory's Supercomputing and Visualization Facility is gratefully acknowledged.

References

[1] L. Sanche, Eur. Phys. J. D35 (2005) 367–390.
[2] Y. Zheng, P. Cloutier, D.J. Hunting, J.R. Wagner, L. Sanche, J. Chem. Phys. 124 (2006) 064710-1–9.
[3] R. Barrios, P. Skurski, J. Simons, J. Phys. Chem. B 106 (2002) 7991–7994.
[4] J. Berdys, I. Anusiewicz, P. Skurski, J. Simons, J. Phys. Chem. A 108 (2004) 2999–3005.
[5] J. Berdys, P. Skurski, J. Simons, J. Phys. Chem. B 108 (2004) 5800–5805.
[6] I. Anusiewicz, J. Berdys, M. Sobczyk, P. Skurski, J. Simons, J. Phys. Chem. A 108 (2004) 11381–11387.
[7] X. Li, M.D. Sevilla, L. Sanche, J. Am. Chem. Soc. 125 (2003) 13668–13669.
[8] J. Berdys, I. Anusiewicz, P. Skurski, J. Simons, J. Am. Chem. Soc. 126 (2004) 6441–6447.
[9] F. Martin, P.D. Burrow, Z. Cai, P. Cloutier, D. Hunting, L. Sanche, Phys. Rev. Lett. 93 (2004) 068101-1-4.
[10] P. Sulzer, S. Ptasinska, F. Zappa, B. Mielewska, A.R. Milosavljevic, P. Scheier, T.D. Märk, I. Bald, S. Gohlke, M.A. Huels, E. Illenberger, J. Chem. Phys. 125 (2006) 044304-1–6.
[11] I. Bald, J. Kopyra, E. Illenberger, Angew. Chem. Int. Ed. 45 (2006) 4851–4855.
[12] I. Bald, J. Kopyra, I. Dabkowska, E. Antonsson, E. Illenberger, J. Chem. Phys. 126 (2007) 074308-1–7.
[13] C. König, J. Kopyra, I. Bald, E. Illenberger, Phys. Rev. Lett. 97 (2006) 018105-1–4.
[14] K. Aflatooni, A.M. Scheer, P.D. Burrow, J. Chem. Phys. 125 (2006) 054301-1–5.
[15] P.D. Burrow, G.A. Gallup, A. Modelli, J. Phys. Chem. A 112 (2008) 4106–4113.
[16] S. Tonzani, C.H. Greene, J. Chem. Phys. 125 (2006) 094504-1–7.
[17] X. Pan, L. Sanche, Chem. Phys. Lett. 421 (2006) 404–408.
[18] M.W. Schmidt, K.K. Baldridge, J.A. Boatz, S.T. Elbert, M.S. Gordon, J.H. Jensen, S. Koseki, N. Matsunaga, K.A. Nguyen, S.J. Su, T.L. Windus, M. Dupuis, J.A. Montgomery, J. Comput. Chem. 14 (1993) 1347–1363.
[19] K. Takatsuka, V. McKoy, Phys. Rev. A 24 (1981) 2473–2480.
[20] K. Takatsuka, V. McKoy, Phys. Rev. A 30 (1984) 1734–1740.
[21] C. Winstead, V. McKoy, Comput. Phys. Commun. 128 (2000) 386–398.
[22] C.W. Bauschlicher, J. Chem. Phys. 72 (1980) 880–885.
[23] M.A. Khakoo, J. Blumer, K. Keane, C. Campbell, H. Silva, M.C.A. Lopes, C. Winstead, V. McKoy, R.F. da Costa, L.G. Ferreira, M.A.P. Lima, M.H.F. Bettega, Phys. Rev. A 77 (2008) 042705-1–10.